Dynamic Surface Control Techniques Applied to Horizontal Position Control of a Quadrotor

Zhilong Liu
Dept. of Civil and Environmental Engineering
University of California, Berkeley
Berkeley California 94720, USA
Email: lzl200102109@berkeley.edu

Karl Hedrick
Dept. of Mechanical Engineering
University of California, Berkeley
Berkeley California 94720, USA
Email: khedrick@me.berkeley.edu

***Abstract*—This paper introduces dynamic surface control (DSC) techniques to formulate concise sliding mode controllers to control the horizontal position of an underactuated quadrotor. Sliding mode control is a popular type of robust nonlinear control method. However, traditional methods on handling underactuated model such as integrator backstepping and dynamic input augmentation could lead to the explosion of terms when time derivatives are taken in controller designs. It makes sliding mode controllers only feasible for highly simplified dynamic models. We solve the term explosion problem by introducing DSC filters in synthetic controls, so that a full quadrotor model can be used for horizontal controller designs.**

I. Introduction

Unmanned Aerial Vehicles (UAVs) are becoming increasing capable on performing autonomous tasks due to the recent advance in sensor technologies. Among various types of UAVs, quadrotors are popular because they are capable of vertical take-off and landing. In addition, quadrotors have hovering capability and omni-directional maneuverability, which enable them to perform tasks such as filming, structural health monitoring, and package delivery.

However, to control a quadrotor, especially in horizontal motions, is non-trivial due to its nonlinear and underactuated nature. Moreover, model uncertainties in payloads and wind make the control even more challenging. To handle the uncertainties, we could use either robust or adaptive control methods. However, there are no concise solutions to the underactuation issue in the control literature. In this paper, we propose a control scheme which combines sliding mode controllers with dynamic surface control (DSC) techniques, to enable robust horizontal position control of a full quadrotor model. This technique also combines well with feedback linearization (FB), but it is not robust to uncertainty and thus not presented.

II. Literature Review

The quadrotor control literature can be divided into two classes. The first class focuses on attitude and altitude stabilization [1]–[5], while the second class controls the horizontal position as well [6]–[8]. Controlling the first class is straight forward because attitude and altitude are directly controlled by four independent control inputs. However, when horizontal position tracking is required, the problem becomes more difficult due to the underactuated nature of quadrotors. In this section, we review both classes of control methods and lead to our contribution.

Attitude and altitude stabilization of a quadrotor could be achieved by many approaches. Classical methods were examined in several papers. In [1], a PID controller and a LQ controller were compared. The PID controller neglected gyroscopic effects but were able to stabilize the system with minor disturbances. The LQ controller gave average performance because the linearized reference model was imperfect. In [2], Li presented another experiment to confirm the feasibility of PID designs. Nonlinear control methods were also widely experimented. In [4], a backstepping and a sliding mode controllers were compared. The backstepping controller gives more robust performance. In [5], an adaptive sliding mode controller was presented. Simulation results indicated that the controller was robust to model uncertainty in mass and rotational inertia.

However, the feasible control methods reduce dramatically when horizontal position tracking is required. The challenge is on resolving the underactuation issue, or using only four independent actuation inputs to handle all six degrees of freedom. Specifically, the tilting in roll and pitch are coupled with horizontal motions. To derive feasible horizontal control laws, the dynamic model is usually greatly simplified [6], [7] to avoid the explosion of terms when taking time derivatives.

In [7], Xu divided the model into two subsystems. The fully actuated system were handled by PID controllers. The underactuated system with horizontal motions was stabilized to a fixed point by a sliding mode controller. However, it was unable to track a moving trajectory because it lacked the time derivatives of the desired roll and pitch. In [6], Lee tried both feedback linearization and adaptive sliding mode to fully control a quadrotor. In feedback linearization, the system was reduced to include only thrust forces and gravity, and yet the derived control laws were quite lengthy. In addition, it augmented the state-space model with control inputs as additional states, yielding complicated dynamical input control laws. In the sliding mode controller, the horizontal position were controlled by two PD controllers, instead. In [8], another similar feedback linearization method with dynamic inputs was presented. Compared to [6], the model in [8] was more complete, and the term explosion problem became huge! In summary, it is practically impossible to derive concise control

978-1-5090-2720-0/16/$31.00 ©2016 IEEE

laws from a full quadrotor model by directly applying nonlinear control methods.

In this paper, we augment the quadrotor model with two first-order filters from the dynamic surface control (DSC) literature [9]. With the DSC filters, we were able to access lagged version of the required time derivatives and indirectly formulate concise control laws, to fully control a quadrotor, including horizontal positions.

III. Dynamic Model

The dynamic model of a quadrotor is similar to a typical airplane with a different set of forces. Here we use Euler angles instead of quaternion, to express the control laws derived later. One limitation of using Euler angles is that there is a singularity at $\theta = 90°$. Define a fixed north-east-down (NED) inertial world frame $\mathcal{W}$ and a non-inertial body frame $\mathcal{B}$ attached to the center of gravity of the quadrotor (Figure 1). The following is a list of variables used to describe the dynamics of a quadrotor.

- $\boldsymbol{X} = [X\ Y\ Z]^T$: quadrotor position in $\mathcal{W}$;
- $\boldsymbol{x} = [x\ y\ z]^T$: quadrotor position in $\mathcal{B}$;
- $\boldsymbol{V} = [V_X\ V_Y\ V_Z]^T$: quadrotor velocity in $\mathcal{W}$;
- $\boldsymbol{\Theta} = [\phi\ \theta\ \psi]^T$: Euler angles roll, pitch, and yaw in $\mathcal{B}$, respectively;
- $\boldsymbol{\omega} = [\omega_x\ \omega_y\ \omega_z]^T$: quadrotor angular velocity in $\mathcal{B}$;
- m: quadrotor mass;
- $\boldsymbol{I} = diag(I_x, I_y, I_z)$: mass moment of inertia in $\mathcal{B}$;
- ω_{r_i}: motor speeds, $i = 1, 2, 3, 4$;
- $\Omega = -\omega_{r_1} + \omega_{r_2} - \omega_{r_3} + \omega_{r_4}$: sum of motor speeds;
- k_f, k_m: motor thrust and torque coefficients, respectively;
- c_t, c_r: translational and rotational drag coefficients, respectively;
- l: moment arm from the origin of $\mathcal{B}$ to each motor.
- $\boldsymbol{g}$: gravitational acceleration, $[0\ 0\ g]^T$ in NED frame with $g = 9.81 m/s^2$.

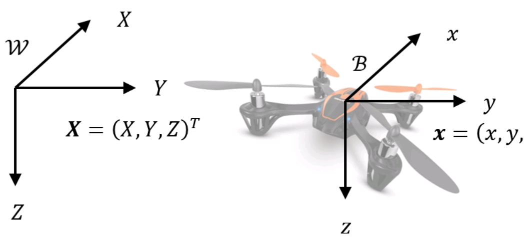

Fig. 1: The reference frames of a quadrotor.

Assume that the motor forces are proportional to motor speed squared $\omega_{r_i}^2$, and the control inputs $\boldsymbol{U}$ satisfy equation (1) with constraints. Physically, the control inputs $U_1, U_2 l, U_3 l, U_4$ represent the total thrust and the total motor torques along the roll, pitch, and yaw axes, respectively. These are the control inputs for altitude and Euler angles. The constraints in (1) represent the physical capacity of the motors.

$$
\boldsymbol{U} = \begin{bmatrix} U_1 \\ U_2 \\ U_3 \\ U_4 \end{bmatrix} = \begin{bmatrix} k_f & k_f & k_f & k_f \\ 0 & k_f & 0 & -k_f \\ k_f & 0 & -k_f & 0 \\ k_m & -k_m & k_m & -k_m \end{bmatrix} \begin{bmatrix} \omega_{r_1}^2 \\ \omega_{r_2}^2 \\ \omega_{r_3}^2 \\ \omega_{r_4}^2 \end{bmatrix}
\tag{1}
$$

$$
\begin{aligned}
4k_f\omega_{r,min}^2 < U_1 \le 4k_f\omega_{r,max}^2 \\
-k_f\omega_{r,max}^2 \le U_2 \le k_f\omega_{r,max}^2 \\
-k_f\omega_{r,max}^2 \le U_3 \le k_f\omega_{r,max}^2 \\
-2k_m\omega_{r,max}^2 \le U_4 \le 2k_m\omega_{r,max}^2
\end{aligned}
$$

Other forces include gravity mg, translation drag $c_t\boldsymbol{V}$, rotational drag $c_r\boldsymbol{\omega}^2$, and Coriolis forces from quadrotor body rotation and motor rotations. The state-space model could be written compactly as equation (2).

$$
\begin{aligned}
\dot{\boldsymbol{X}} &= \boldsymbol{V} \\
\dot{\boldsymbol{\Theta}} &= R_v^{-1}\boldsymbol{\omega} \\
\dot{\boldsymbol{V}} &= \boldsymbol{g} + \frac{1}{m}\left(-c_t\boldsymbol{V} - R_{\mathcal{B}\to\mathcal{W}}\begin{bmatrix} 0 \\ 0 \\ U_1 \end{bmatrix}\right) \\
\dot{\boldsymbol{\omega}} &= I^{-1}\left(\boldsymbol{\omega} \times (I\boldsymbol{\omega}) - \boldsymbol{\omega} \times \left(I_r \begin{bmatrix} 0 \\ 0 \\ \Omega \end{bmatrix}\right) - c_r\boldsymbol{\omega}^2 + \begin{bmatrix} U_2 l \\ U_3 l \\ U_4 \end{bmatrix}\right)
\end{aligned}
\tag{2}
$$

In (2), $R_{\mathcal{B}\to\mathcal{W}}$ is the rotation matrix from frame $\mathcal{B}$ to $\mathcal{W}$, and R_v is a linear transformation from $\dot{\boldsymbol{\Theta}}$ to $\boldsymbol{\omega}$. Use small case s and c to respresent sin and cos functions, respectively, then the matrices are given by

$$
R_{\mathcal{B}\to\mathcal{W}} = \begin{bmatrix} c\theta c\psi & s\phi s\theta c\psi - c\phi s\psi & c\phi s\theta c\psi + s\phi s\psi \\ c\theta s\psi & s\phi s\theta s\psi + c\phi c\psi & c\phi s\theta s\psi - s\phi c\psi \\ -s\theta & s\phi c\theta & c\phi c\theta \end{bmatrix}
$$

$$
R_v = \begin{bmatrix} 1 & 0 & -s\theta \\ 0 & c\phi & s\phi c\theta \\ 0 & -s\phi & c\phi c\theta \end{bmatrix}
$$

We only gives a brief summary of the model to introduce enough notations for controller derivations. For details, refer to an equivalent dynamic model in [5]. The expanded version of (2) is given by equation (17) at the end of the paper for derivation reference.

IV. Position Controllers

Given the quadrotor model in Section III, we can follow the standard procedure of designing sliding mode controllers, and formulate four independent control laws governing the altitude and attitudes (Euler angles) [5]. However, to achieve horizontal position control, we need to derive the desired roll (ϕ_d) and pitch (θ_d) as intermediate bridges. On one hand, they serve as synthetic control inputs for horizontal motions in X and Y. On the other hand, they are also the reference signals for the actual roll (ϕ) and pitch (θ). As is mentioned before, traditional methods such as backstepping and state augmentation lead to explosion of terms. To avoid that, we apply dynamic surface control (DSC) techniques in the horizontal position controllers.

First, we define the tracking errors. We use the subscript $_d$ to represent the desired value of any variable.

$$
\begin{aligned}
e_X &\triangleq X - X_d & e_\theta &\triangleq \theta - \theta_d \\
e_Y &\triangleq Y - Y_d & e_\phi &\triangleq \phi - \phi_d \\
e_Z &\triangleq Z - Z_d & e_\psi &\triangleq \psi - \psi_d
\end{aligned}
$$

Note that to achieve position control, we can specify the desired position (X_d, Y_d, Z_d) and desired yaw (ψ_d). However, we cannot arbitrarily specify the desired pitch (θ_d) and roll (ϕ_d) because they are coupled with the horizontal motions (X_d, Y_d).

Define the sliding surfaces to be some first-order filters of the error terms (3) with tuning parameters $\lambda's$ [10]. Note that the first terms in S_ϕ and S_θ are different from the rest.

$$
\begin{aligned}
S_X &\triangleq \dot{e}_X + \lambda_X e_X & S_\theta &\triangleq \dot{\theta} + \lambda_\theta e_\theta \\
S_Y &\triangleq \dot{e}_Y + \lambda_Y e_Y & S_\phi &\triangleq \dot{\phi} + \lambda_\phi e_\phi \\
S_Z &\triangleq \dot{e}_Z + \lambda_Z e_Z & S_\psi &\triangleq \dot{e}_\psi + \lambda_\psi e_\psi
\end{aligned} \tag{3}
$$

The asymptotic stability proof of a general sliding mode controller is based on Lyapunov's second method. Define a general sliding surface S in a form similar to (3). First, we compute $\dot{S}$, or the time derivative of S, and set it equal to $-\eta sgn(S)$. Let the positive definite Lyapunov function be $V = \frac{1}{2}S^2$, then $\dot{V} = S\dot{S} \leq -\eta|S|$ is negative definite, which guarantees $S \to 0$ asymptotically. Once we are on $S = 0$, the tracking error goes to zero exponentially [11]. Here, we simply use the design method without proofs.

A. Vertical and Yaw Controllers

The sliding mode controllers for altitude and yaw are straight-forward. Take the first time derivatives of the corresponding sliding surfaces in (3), and set them equal to the robustness terms with parameters η_Z and η_ψ, we have

$$
\begin{aligned}
\dot{S}_Z &= (\dot{V}_Z - \ddot{X}_d) + \lambda_Z \dot{e}_Z \triangleq -\eta_Z sgn S_Z \\
\dot{S}_\psi &\approx (\dot{\omega}_z - \ddot{\psi}_d) + \lambda_\psi \dot{e}_\psi \triangleq -\eta_\psi sgn S_\psi
\end{aligned} \tag{4}
$$

In (4), we approximate $\ddot{\psi}$ to be $\dot{\omega}_z$. Substitute $\dot{V}_Z$ and $\dot{\omega}_z$ from (17) into (4), we get the vertical and yaw control laws in (5).

$$
\begin{aligned}
U_1 &= \frac{m}{c\phi c\theta}\left[\left(-g + \frac{c_t}{m}V_Z + \ddot{Z}_d\right) - \lambda_Z \dot{e}_Z - \eta_Z sgn S_Z\right] \\
U_4 &= I_z\left[\left(-\frac{I_x - I_y}{I_z}\omega_x\omega_y + \frac{c_r}{I_z}\omega_z^2 + \ddot{\psi}_d\right) - \lambda_\psi \dot{e}_\psi - \eta_\psi sgn S_\psi\right]
\end{aligned} \tag{5}
$$

B. Horizontal Controllers

In this section, we derive the horizontal control laws by augmenting our system with DSC filters. The overall horizontal motion control architecture is shown in Figure 2. It is a 3-step process. First, we derive the synthetic controls $\bar{\theta}$ and $\bar{\phi}$ required to track X_d and Y_d via sliding mode. At this point, if we use U_3 and U_2 to control $\bar{\theta}$ and $\bar{\phi}$ directly, we will have to take time derivatives of $\bar{\theta}$ and $\bar{\phi}$ and lead to the explosion of terms. Instead, we convert $\bar{\theta}$ and $\bar{\phi}$ into θ_d and ϕ_d, respectively, using DSC filters. The derivatives of θ_d and ϕ_d are implicitly given by the filter updates and thus resolved the term explosion problem. Finally, we can use control inputs U_3 and U_2 to drive θ and ϕ to θ_d and ϕ_d, respectively, via sliding mode. In the following, we show the design process in details.

$$
\begin{bmatrix} X_d \\ Y_d \end{bmatrix} \overset{SM}{\longleftarrow} \begin{bmatrix} \bar{\theta} \\ \bar{\phi} \end{bmatrix} \overset{DSC}{\longleftarrow} \begin{bmatrix} \theta_d \\ \phi_d \end{bmatrix} \overset{SM}{\longleftarrow} \begin{bmatrix} U_3 \\ U_2 \end{bmatrix}
$$

Fig. 2: The horizontal motion control architecture.

1) derive synthetic inputs $\bar{\theta}$ and $\bar{\phi}$ via sliding mode: First, take the time derivative of the sliding surfaces S_X and S_Y in (3) and set them equal to the robustness terms with parameters η_X and η_Y, respectively.

$$
\begin{aligned}
\dot{S}_X &= (\dot{V}_X - \ddot{X}_d) + \lambda_X \dot{e}_X \triangleq -\eta_X sgn S_X \\
\dot{S}_Y &= (\dot{V}_Y - \ddot{Y}_d) + \lambda_Y \dot{e}_Y \triangleq -\eta_Y sgn S_Y
\end{aligned} \tag{6}
$$

Substitute $\dot{V}_X$ and $\dot{V}_Y$ from (17) into (6) and simplify, we have

$$
R(\psi)\begin{bmatrix} c\phi s\theta \\ s\phi \end{bmatrix} = \begin{bmatrix} \frac{m}{U_1}\left(\left(\frac{c_t}{m}V_X + \ddot{X}_d\right) - \lambda_X \dot{e}_X - \eta_X sgn S_X\right) \\ \frac{m}{U_1}\left(\left(\frac{c_t}{m}V_Y + \ddot{Y}_d\right) - \lambda_Y \dot{e}_Y - \eta_Y sgn S_Y\right) \end{bmatrix} \tag{7}
$$

where the matrix $R(\psi)$ is

$$
R(\psi) \triangleq \begin{bmatrix} c\psi & s\psi \\ s\psi & -c\psi \end{bmatrix}
$$

Note that the roll ϕ and pitch θ on the left-hand side of equation (7) actually represent the synthetic controls for the desired horizontal motions. We denote these two synthetic controls as $\bar{\theta}$ and $\bar{\phi}$ to distinguish them from the actual pitch θ and roll ϕ. We can further simplify (7) with small angle approximations: $c\phi s\theta \approx \theta$ and $s\phi \approx \phi$, yielding sliding mode control laws (8).

$$
\begin{bmatrix} \bar{\theta} \\ \bar{\phi} \end{bmatrix} = R(\psi)\begin{bmatrix} \frac{m}{U_1}\left(\left(\frac{c_t}{m}V_X + \ddot{X}_d\right) - \lambda_X \dot{e}_X - \eta_X sgn S_X\right) \\ \frac{m}{U_1}\left(\left(\frac{c_t}{m}V_Y + \ddot{Y}_d\right) - \lambda_Y \dot{e}_Y - \eta_Y sgn S_Y\right) \end{bmatrix} \tag{8}
$$

2) augment system with DSC filters: To proceed, we need to somehow use equation (8) in the time derivative of S_θ and S_ϕ, so that the controls U_3 and U_2 can appear. However, as was mentioned in Section II, it requires taking time derivatives of (8), which leads to explosion of terms. To avoid that, we instead augment the dynamic system (2) with two first-order DSC filters shown in (9), to indirectly converge the desired pitch θ_d and roll ϕ_d to the synthetic controls $\bar{\theta}$ and $\bar{\phi}$, respectively [9]. The time constants τ_θ and τ_ϕ determine the convergence rates. The initial conditions are set to zeros in both filters.

$$\begin{aligned} \tau_\theta \dot{\theta}_d + \theta_d = \bar{\theta}, \quad \theta_d(0) = 0 \\ \tau_\phi \dot{\phi}_d + \phi_d = \bar{\phi}, \quad \phi_d(0) = 0 \end{aligned} \tag{9}$$

The DSC filters (9) allows us to compute $\dot{\theta}_d$ and $\dot{\phi}_d$ required in $\dot{S}_\theta$ and $\dot{S}_\phi$, without taking time derivatives of $\bar{\theta}$ and roll $\bar{\phi}$. Therefore, no simplifications in the dynamics are needed to accommodate the explosion of terms. A semi-global stability proof via Lyapunov analysis is lengthy because it involves the error dynamics $(\dot{\theta}_d - \dot{\bar{\theta}})$ and $(\dot{\phi}_d - \dot{\bar{\phi}})$, which again involve explosion of terms. A standard proof is provided in [9]. Here, we simply adopt the results.

3) derive control inputs U_3 and U_2 via sliding mode: Now we can take the time derivatives of S_θ and S_ϕ, and set them equal to their robustness terms with parameters η_θ and η_ϕ, respectively, with $\ddot{\theta} \approx \dot{\omega}_y$ and $\ddot{\phi} \approx \dot{\omega}_x$.

$$\begin{aligned} \dot{S}_\theta \approx \dot{\omega}_y + \lambda_\theta(\dot{\theta} - \dot{\theta}_d) \stackrel{\triangle}{=} -\eta_\theta sgn S_\theta \\ \dot{S}_\phi \approx \dot{\omega}_x + \lambda_\phi(\dot{\phi} - \dot{\phi}_d) \stackrel{\triangle}{=} -\eta_\phi sgn S_\phi \end{aligned} \tag{10}$$

In equation (10), $\dot{\omega}_y$ and $\dot{\omega}_x$ include the control inputs U_3 and U_2. They ($\dot{\omega}_y$ and $\dot{\omega}_x$), as well as $\dot{\theta}$ and $\dot{\phi}$, are given by (17), and $\dot{\theta}_d$ and $\dot{\phi}_d$ are given by re-expressing the DSC filters as (11).

$$\begin{aligned} \dot{\theta}_d &= \frac{1}{\tau_\theta}\left(\bar{\theta} - \theta_d\right) \\ \dot{\phi}_d &= \frac{1}{\tau_\phi}\left(\bar{\phi} - \phi_d\right) \end{aligned} \tag{11}$$

In equation (11), $\bar{\theta}$ and $\bar{\phi}$ are given by (8), and θ_d and ϕ_d are given by the DSC filter updates in (9). Then, the horizontal control laws are given by

$$\begin{aligned} U_3 = \frac{I_y}{l}\left[\left(-\frac{I_z - I_x}{I_y}\omega_x\omega_z + \frac{c_r}{I_y}\omega_y^2 + \frac{I_r}{I_y}\Omega\omega_x\right) - \lambda_\theta \dot{e}_\theta - \eta_\theta sgn S_\theta\right] \\ U_2 = \frac{I_x}{l}\left[\left(-\frac{I_y - I_z}{I_x}\omega_y\omega_z + \frac{c_r}{I_x}\omega_x^2 + \frac{I_r}{I_x}\Omega\omega_y\right) - \lambda_\phi \dot{e}_\phi - \eta_\phi sgn S_\phi\right] \end{aligned} \tag{12}$$

Note that the terms in (5), (8) and (12) could be categorized into three parts. Take U_1 as an example. The first part $\left(-g + \frac{c_t}{m}V_Z + \ddot{Z}_d\right)$ cancels the original (possibly nonlinear) dynamics; the second part $(-\lambda_Z \dot{e}_Z)$ is the desired linear dynamics; the third part $(-\eta_Z sgn S_Z)$ is an uncertainty robustness term.

Lastly, the signum function ($sgn(\cdot)$) should be replaced by a smoothed function to avoid chattering. In this paper, we use a function with logistic and linear smoothing (13).

$$\eta sgn(S) \leftarrow \left[\eta_1\left(\frac{2}{1+e^{-cS}} - 1\right) + \eta_2 S\right] \tag{13}$$

Other than small angle approximations, we did not make any simplification to the full dynamic model (2) throughout the derivations. The innovation lies in the adoption of DSC filters.

V. Simulations

In this section, we present the simulation results of the sliding mode controllers. First, we examine the behavior of the sliding mode controllers with DSC filters defined in equation (9). Second, the robustness of the sliding mode controllers is evaluated with respect to disturbance, model uncertainty, and measurement noise. All simulations are performed in MATLAB/SIMULINK R2015a [12] with a fixed-time-step solver $dt = 0.002sec$.

The quadrotor parameters are referenced from [13] with a different rotational inertia matrix, so that the model is more realistic.

$$\begin{aligned} m &= 2.0\ kg & \boldsymbol{g} &= [0\ 0\ 9.81]^T\ m/s^2 \\ k_m &= 10^{-6}\ Nm \cdot s^2 & k_f &= 10^{-5}\ N \cdot s^2 \\ c_t &= 10^{-2}\ Ns/m & c_r &= 10^{-2}\ Nm \cdot s^2 \\ l &= 0.2m & I &= 1.2416\ diag([1\ 1\ 2]e\text{-}2)\ kg\ m^2 \end{aligned} \tag{14}$$

The reference trajectories in altitude, yaw, and horizontal positions are either sinusoids or zeros. The sinusoidal references are taken from [14] in equation (15). The exponential terms are introduced to produce smooth initial references.

$$\begin{aligned} X_d(t) &= (1 - e^{-t^3}) sint\ m \\ Y_d(t) &= (1 - e^{-t^3}) cost\ m \\ Z_d(t) &= -(1 - e^{-t^3})\ m \\ \psi_d(t) &= 30(1 - e^{-t^3}) sint\ ^\circ \end{aligned} \tag{15}$$

The controller gains are listed below in (16). There are two sets of $\eta's$ as defined in (13) for each of the six control laws (5), (8), and (12). The two time constants τ_ϕ and τ_θ are chosen to minimize filter lags while preserving system stability.

$$\begin{array}{lll} \eta_{1X} = 3 & \eta_{1Y} = 3 & \eta_{1Z} = 4 \\ \eta_{1\phi} = 20 & \eta_{1\theta} = 20 & \eta_{1\psi} = 10 \\ \eta_{2X} = 1 & \eta_{2Y} = 1 & \eta_{2Z} = 5 \\ \eta_{2\phi} = 50 & \eta_{2\theta} = 50 & \eta_{2\psi} = 10 \\ \lambda_X = 2 & \lambda_Y = 2 & \lambda_Z = 3 \\ \lambda_\phi = 50 & \lambda_\theta = 50 & \lambda_\psi = 10 \\ c_X = 5 & c_Y = 5 & c_Z = 50 \\ c_\phi = 80 & c_\theta = 80 & c_\psi = 10 \\ \tau_\phi = 0.1 & \tau_\theta = 0.1 & \end{array} \tag{16}$$

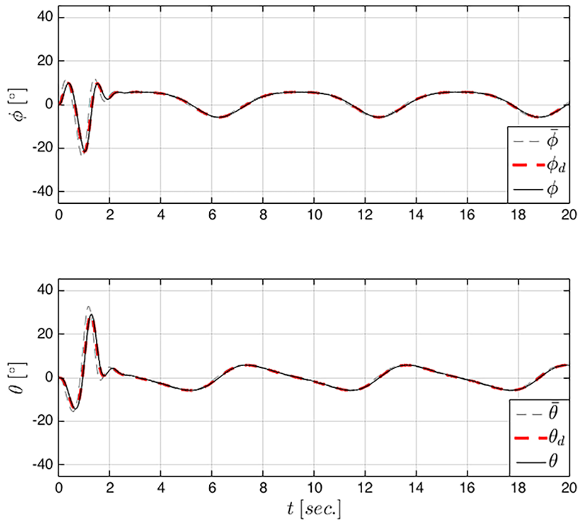

(a) DSC filters make ϕ_d and θ_d (dashed red lines) follow $\bar{\phi}$ and $\bar{\theta}$ (dashed gray lines) with small lags, respectively. Then, sliding mode controllers in (12) drive θ and ϕ (solid black lines) to θ_d and ϕ_d, respectively.

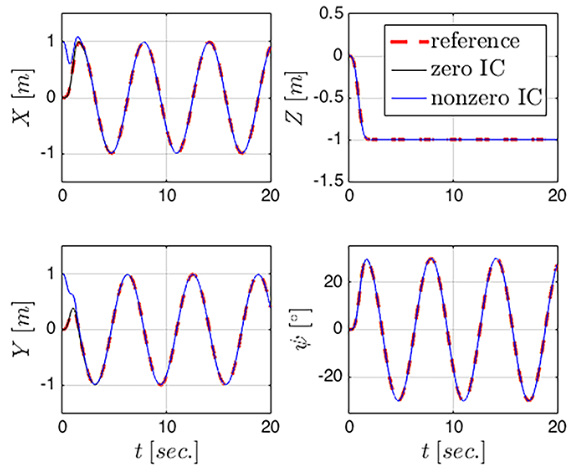

(b) tracking reference signals with zero (solid black lines) and nonzero (solid blue lines) initial conditions (IC).

Fig. 3: Tracking performance without disturbance.

A. Behavior of the sliding mode controllers with DSC filters

Figure 3 shows the tracking performance of both the DSC filters and sliding mode controllers without any model uncertainties or disturbances. In Figure 3a, the gray dashed lines indicate the synthetic controls $\bar{\phi}$ and $\bar{\theta}$ required to drive the quadrotor to a desired horizontal position (X_d, Y_d) (equation (8)). To use sliding mode control, we need the derivatives of $\bar{\phi}$ and $\bar{\theta}$. However, if their derivatives were computed analytically from equation (8), we would have explosion of terms. Instead, by introducing the DSC filters, the reference synthetic controls ϕ_d and θ_d in dashed red lines (equation (9)) are able to track $\bar{\phi}$ and $\bar{\theta}$ closely with only small lags. As a result, we can compute their derivatives from equation (11) analytically. With ϕ_d, θ_d, and their derivatives, the sliding mode controllers in (12) can drive the quadrotor roll (ϕ) and pitch (θ) to θ_d and ϕ_d, respectively. Therefore, horizontal position tracking is achieved.

Figure 3b shows the tracking results of a perfectly known quadrotor model, with respect to zero or nonzero initial conditions (IC). In the case with zero IC (black), we have almost perfect tracking for all references. In the case with nonzero horizontal IC, the convergence in X and Y is also fast, both within $3sec$.

B. Robustness evaluation of the sliding mode controllers with DSC filters

1) disturbance: The disturbance model is an external wind field $\boldsymbol{V_{wind}} = [10\ 10\ 10]m/s$ similar to [3], applied right after time $t = 5sec$. To examine the disturbance effect, we used zero references for X, Y, and Z, instead. Figure 4a shows that the horizontal and vertical trackings are affected by about $10^{-3}m$ and $10^{-4}m$, respectively. The tracking errors could not be eliminated because we smoothed the signum functions to avoid chattering. The results are acceptable because the errors are so tiny and would not be noticeable.

2) model uncertainty: We examined the robustness of model uncertainty by varying mass m and rotational inertia RI [5]. We first considered an uncertainty of 20% on mass and 10% on RI, and second an uncertainty of 35% on mass and 15% on RI. The tracking references are given by (15). Figure 4b shows the simulation results. The difference in performance could not be observed in the overall tracking plots. When zoomed in (gray boxes), we can see that the altitude tracking is affected by $0.005m$ to $0.010m$ due to mass uncertainty, and the horizontal tracking is affected by about $0.01m$ due to both mass and RI uncertainty. Again, the additional tracking errors due to mass and RI are quite small. The controllers are robust to mass and RI uncertainty.

3) measurement noise: Lastly, we examined to robustness to measurement noise by inserting white Gaussian noise (18) (in SI units) [15] into the 12 states given by (2). The MATLAB command $randn(12,1)$ generates a noise vector of 12 elements with mean 0 and standard deviation (SD) 1. Then, the noise vector is vector multiplied by the desired SD's. The references are again given by (15).

$$\begin{aligned} Noise = randn(12,1)([10;\ 10;\ 10;\ 1;\ 1;\ 1; \\ 10;\ 10;\ 10;\ 1;\ 1;\ 1]10^{-2}) \end{aligned} \tag{18}$$

The simulation results are shown in Figure 4c. The tracking of the first 2 to $3sec$ are affected slightly by noise. The zoomed in view in Z shows the noisy trajectory with an average error of about $0.001m$ (blue line). Yaw tracking becomes a little noisy but is essentially unchanged. Interestingly, observe that the X and Y tracking trajectories are still smooth under noisy measurements. It is due to the smoothing effect of the DSC filters, which could be observed in Figure 5. The controllers are robust to measurement noise.

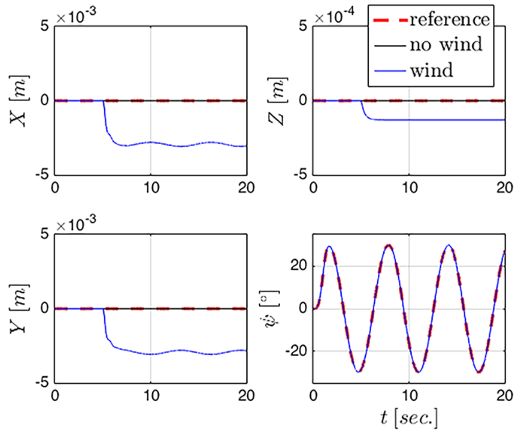

(a) constant wind disturbance

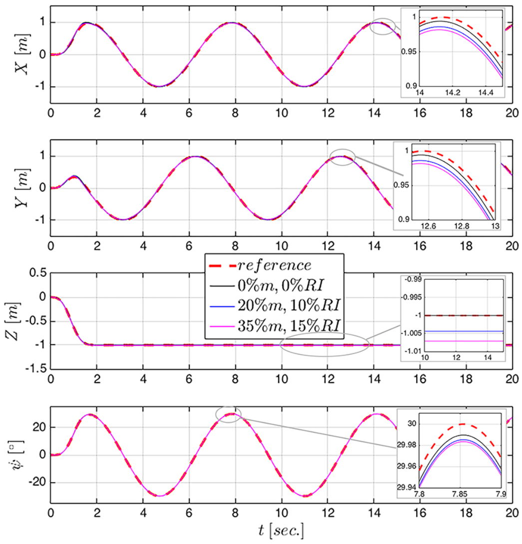

(b) mass and rotational inertia (RI) uncertainty

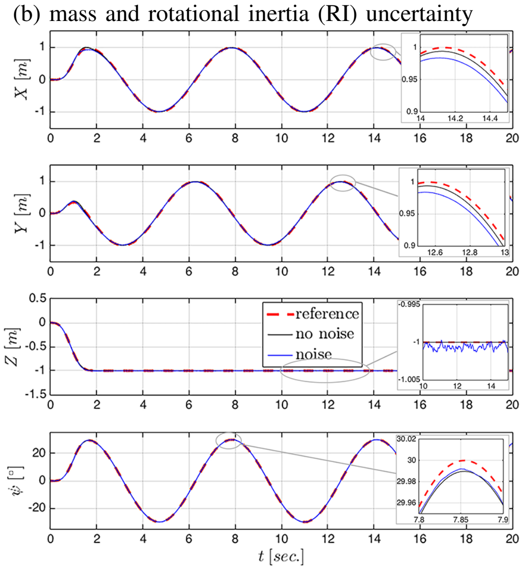

(c) measurement noise

Fig. 4: Tracking performance with model uncertainty, disturbance, and measurement noise.

VI. Conclusions

In this paper, we introduce DSC filters to overcome the term explosion problem in sliding mode control of an underactuated quadrotor. This technique is also applicable to other nonlinear control methods, i.e. feedback linearization. The filters introduce small lags but facilitate us to obtain time derivatives of complex intermediate signals. The controllers were first simulated under unmatched initial conditions in a perfect model. Simulation indicated fast convergence to all reference signals. The robustness of the controllers were tested under wind disturbance, mass uncertainty, and measurement noise. The controllers performs very well in all tests. In the future, we would like to make the controllers adaptive to model uncertainty and varying wind disturbance.

Acknowledgment

This research was supported by the University Affiliated Research Center (UARC) at NASA Ames (Contract number: UCSCMCA-14-020) and the National Science Foundation (NSF) (Contract number: CNS-1136141). I also would like to thank Prof. Karl Hedrick for providing his expertise in this project.

References

[1] S. Bouabdallah, A. Noth, and R. Siegwart, "PID vs LQ control techniques applied to an indoor micro quadrotor," in *Intelligent Robots and Systems, 2004.(IROS 2004). Proceedings. 2004 IEEE/RSJ International Conference on*, vol. 3. IEEE, 2004, pp. 2451–2456.

[2] J. Li and Y. Li, "Dynamic analysis and pid control for a quadrotor," in *Mechatronics and Automation (ICMA), 2011 International Conference on*. IEEE, 2011, pp. 573–578.

[3] T. Madani and A. Benallegue, "Backstepping sliding mode control applied to a miniature quadrotor flying robot," in *IEEE Industrial Electronics, IECON 2006-32nd Annual Conference on*. IEEE, 2006, pp. 700–705.

[4] S. Bouabdallah and R. Siegwart, "Backstepping and sliding-mode techniques applied to an indoor micro quadrotor," in *Robotics and Automation, 2005. ICRA 2005. Proceedings of the 2005 IEEE International Conference on*. IEEE, 2005, pp. 2247–2252.

[5] H. Bouadi, S. S. Cunha, A. Drouin, and F. Mora-Camino, "Adaptive sliding mode control for quadrotor attitude stabilization and altitude tracking," in *Computational Intelligence and Informatics (CINTI), 2011 IEEE 12th International Symposium on*. IEEE, 2011, pp. 449–455.

[6] D. Lee, H. J. Kim, and S. Sastry, "Feedback linearization vs. adaptive sliding mode control for a quadrotor helicopter," *International Journal of control, Automation and systems*, vol. 7, no. 3, pp. 419–428, 2009.

[7] R. Xu and Ü. Özgüner, "Sliding mode control of a quadrotor helicopter," in *Decision and Control, 2006 45th IEEE Conference on*. IEEE, 2006, pp. 4957–4962.

[8] T. Taniguchi, L. Eciolaza, and M. Sugeno, "Quadrotor control using dynamic feedback linearization based on piecewise bilinear models," in *Computational Intelligence in Control and Automation (CICA), 2014 IEEE Symposium on*. IEEE, 2014, pp. 1–7.

[9] B. Song and J. K. Hedrick, *Dynamic surface control of uncertain nonlinear systems: an LMI approach*. Springer Science & Business Media, 2011.

[10] J.-J. E. Slotine, W. Li *et al.*, *Applied nonlinear control*. Prentice-Hall Englewood Cliffs, NJ, 1991, vol. 60.

[11] H. K. Khalil, *Nonlinear control*. Prentice Hall, 2014.

[12] MATLAB. [Online]. Available: http://www.mathworks.com/products/matlab/

[13] T. Madani and A. Benallegue, "Backstepping control for a quadrotor helicopter," in *Intelligent Robots and Systems, 2006 IEEE/RSJ International Conference on*. IEEE, 2006, pp. 3255–3260.

$$
\begin{bmatrix} \dot{X} \\ \dot{Y} \\ \dot{Z} \\ \dot{\phi} \\ \dot{\theta} \\ \dot{\psi} \\ \dot{V}_X \\ \dot{V}_Y \\ \dot{V}_Z \\ \dot{\omega}_x \\ \dot{\omega}_y \\ \dot{\omega}_z \end{bmatrix} = \begin{bmatrix} V_X \\ V_Y \\ V_Z \\ \omega_x + \omega_y s\phi tan\theta + \omega_z c\phi tan\theta \\ \omega_y c\phi - \omega_z s\phi \\ -\frac{c_t}{m} V_X \\ -\frac{c_t}{m} V_Y \\ -\frac{c_t}{m} V_Z \\ \frac{I_y - I_z}{I_x}\omega_y\omega_z - \frac{c_r}{I_x}\omega_x^2 - \frac{I_r}{I_x}\Omega\omega_y \\ \frac{I_z - I_x}{I_y}\omega_x\omega_z - \frac{c_r}{I_y}\omega_y^2 - \frac{I_r}{I_y}\Omega\omega_x \\ \frac{I_x - I_y}{I_x}\omega_x\omega_y - \frac{c_r}{I_z}\omega_z^2 \end{bmatrix} + \begin{bmatrix} 0 \\ 0 \\ 0 \\ 0 \\ 0 \\ 0 \\ \frac{c\phi s\theta c\psi + s\phi s\psi}{m} \\ \frac{c\phi s\theta s\psi - s\phi c\psi}{m} \\ \frac{c\phi c\theta}{m} \\ 0 \\ 0 \\ 0 \end{bmatrix} U_1 + \begin{bmatrix} 0 \\ 0 \\ 0 \\ 0 \\ 0 \\ 0 \\ 0 \\ 0 \\ 0 \\ \frac{l}{I_x} \\ 0 \\ 0 \end{bmatrix} U_2 + \begin{bmatrix} 0 \\ 0 \\ 0 \\ 0 \\ 0 \\ 0 \\ 0 \\ 0 \\ 0 \\ 0 \\ \frac{l}{I_y} \\ 0 \end{bmatrix} U_3 + \begin{bmatrix} 0 \\ 0 \\ 0 \\ 0 \\ 0 \\ 0 \\ 0 \\ 0 \\ 0 \\ 0 \\ 0 \\ \frac{1}{I_z} \end{bmatrix} U_4 \qquad (17)
$$

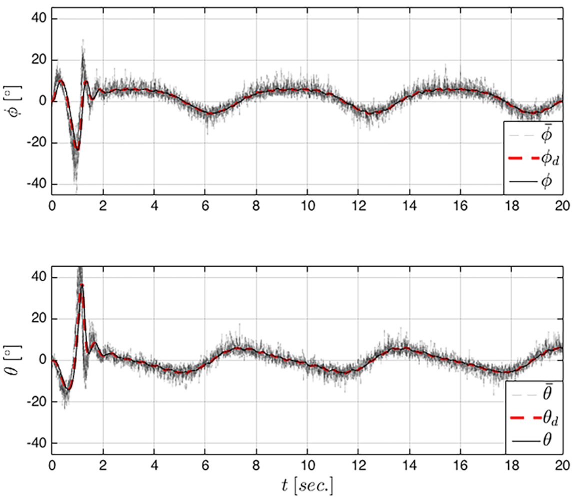

Fig. 5: Synthetic controls with DSC filters under noisy measurements.

[14] M. Huang, B. Xian, C. Diao, K. Yang, and Y. Feng, "Adaptive tracking control of underactuated quadrotor unmanned aerial vehicles via backstepping," in *American Control Conference (ACC), 2010*. IEEE, 2010, pp. 2076–2081.

[15] M. Bouchoucha, M. Tadjine, A. Tayebi, and P. Mullhaupt, "Step by step robust nonlinear pi for attitude stabilisation of a four-rotor mini-aircraft," in *Control and Automation, 2008 16th Mediterranean Conference on*. IEEE, 2008, pp. 1276–1283.